

## On the Calculation of Atomic Forces in Classical Simulation Using the Charge-on-Spring Method To Explicitly Treat Electronic Polarization

Daan P. Geerke and Wilfred F. van Gunsteren\*

Laboratory of Physical Chemistry, Swiss Federal Institute of Technology Zürich  
(ETH), CH-8093 Zürich, Switzerland

Received June 29, 2007

**Abstract:** An expression for the atomic forces in simulations using the charge-on-spring (COS) polarizable model is rederived. In previous implementations of COS-based models, contributions arising from the dependence of the induced dipoles (i.e., the positions of the charges-on-spring) on the coordinates of the other sites in the system were not taken into account. However, from calculations on gas-phase dimers we found a significant contribution of these terms. Errors in the forces when neglecting these contributions in condensed-phase calculations can be significantly reduced by choosing an appropriately large value for the size of the charge-on-spring.

### 1. Introduction

In classical atomistic simulation, electronic polarization effects can be taken into account using polarizable force fields.<sup>1–4</sup> When using such a force field, atomic dipoles or molecular charge distributions can adapt to the electric field generated by the environment to induce a net dipole moment. Several methods have been described in the literature that explicitly treat electronic polarization.<sup>1–4</sup> In one of them, the point-polarizable dipole (PPD) model,<sup>5–7</sup> the polarizable centers  $i$  in the system are assigned an inducible point-dipole  $\vec{\mu}_i$ , which adapts size and direction according to its polarizability  $\alpha_i$  and the electric field  $\vec{E}_i$  at  $i$  (assuming isotropic  $\alpha_i$  and linear dependence of  $\vec{\mu}_i$  on  $\vec{E}_i$ , and using SI units)

$$\vec{\mu}_i = \alpha_i(4\pi\epsilon_0)\vec{E}_i \quad (1)$$

Additionally to the  $U^{qq}$  term to describe Coulomb interactions between the fixed point-charges ( $q_i$ ), the induced dipoles enter the expression for the electrostatic part of the potential energy ( $U^{\text{ele}}$ ) via  $U^{\text{stat}}$ ,  $U^{\mu\mu}$ , and  $U^{\text{self}}$ . The first two terms account for induced dipole–fixed point-charge and induced dipole–induced dipole interactions, respectively<sup>4</sup>

$$U^{\text{ele}}(\vec{r}, \vec{\mu}) = U^{qq} + U^{\text{stat}} + U^{\mu\mu} + U^{\text{self}}$$

$$= \frac{1}{4\pi\epsilon_0} \sum_{i=1}^{N-1} \sum_{j>i}^N \frac{q_i q_j}{|\vec{r}_i - \vec{r}_j|} - \sum_{i=1}^N \vec{\mu}_i \cdot \vec{E}_i^q - \frac{1}{2} \sum_{i=1}^{N-1} \sum_{j>i}^N \vec{\mu}_i \cdot \underline{T}_{ij} \vec{\mu}_j + \sum_{i=1}^N \frac{\vec{\mu}_i \cdot \vec{\mu}_i}{2\alpha_i(4\pi\epsilon_0)} \quad (2)$$

while  $U^{\text{self}}$  is the self-polarization term accounting for the energy cost of dipole induction,<sup>8</sup>  $\vec{E}_i^q$  is the electric field at  $i$  from the fixed point-charges, and  $\underline{T}_{ij}$  are the elements of the dipole tensor.<sup>4</sup> Because the  $\vec{\mu}_i$ 's depend via  $\vec{E}_i$  on the positions of the other point-charges and the sizes of the induced dipoles in the system, the forces at the polarizable centers  $i$  are calculated from

$$\vec{f}_i = -\nabla_i U^{\text{ele}}(\vec{r}, \vec{\mu}) = -\left( \frac{\partial U^{\text{ele}}}{\partial \vec{r}_i} + \sum_{k \neq i}^N \frac{\partial U^{\text{ele}}}{\partial \vec{\mu}_k} \cdot \frac{\partial \vec{\mu}_k}{\partial \vec{r}_i} \right) \quad (3)$$

For a given set of atomic positions, eq 1 can be satisfied by an instantaneous adaptation of the  $\vec{\mu}_i$ 's to the  $\vec{E}_i$ 's. Due to the mutual dependence of the  $\vec{E}_i$ 's and  $\vec{\mu}_i$ 's, an iterative scheme is usually employed<sup>6</sup> to minimize  $U^{\text{ele}}$ , following a Born–Oppenheimer-like approximation<sup>9</sup> to determine the induced dipoles. If the convergence criterion is chosen tightly enough,  $U^{\text{ele}}$  is minimized with respect to the  $\vec{\mu}_i$ 's and

\* Corresponding author fax: (+41)-44-632-1039; e-mail: wfvgn@igc.phys.chem.ethz.ch.

$$\frac{\partial U^{\text{ele}}}{\partial \vec{\mu}_i} = 0 \quad (4)$$

As a result, eq 3 reduces to

$$\vec{f}_i = -\frac{\partial U^{\text{ele}}}{\partial \vec{r}_i} \quad (5)$$

Instead of employing an iterative scheme, simulation studies using the PPD model have been reported<sup>7</sup> in which fictitious masses are assigned to the  $\vec{\mu}_i$ 's. In this case, the  $\vec{\mu}_i$ 's enter the equations of motion via an extended Lagrangian (as in the Car–Parrinello approach<sup>10</sup> to treat electronic degrees of freedom). Thus, forces at the polarizable centers  $i$  can be evaluated as the sum of the term on the right in eq 5 and a term involving  $-\partial U^{\text{ele}}/\partial \vec{\mu}_i$ , although simulation settings are often chosen such that it can be assumed that the components of the  $\vec{\mu}_i$ 's are close enough to their Born–Oppenheimer values to fulfill the condition of eq 4.

As an alternative to the PPD approach, the inducible dipole moments can be described by the charge-on-spring<sup>11</sup> (COS) (or Drude-oscillator<sup>12</sup> or shell<sup>13</sup>) model. In this case, an inducible dipole is modeled by attaching a massless, virtual site with a point-charge  $q_i^v$  to the polarizable center  $i$ , via a spring with harmonic force constant  $k_i^{\text{ho}}$ ,<sup>4</sup>

$$k_i^{\text{ho}} = \frac{(q_i^v)^2}{\alpha_i(4\pi\epsilon_0)} \quad (6)$$

The charge at the polarizable center is then  $(q_i - q_i^v)$ . Thus, the induced dipoles  $\vec{\mu}_i$  are represented by

$$\vec{\mu}_i = q_i^v(\vec{r}_i' - \vec{r}_i) \quad (7)$$

where  $\vec{r}_i'$  is the position of the charge-on-spring. In COS-based schemes in which the charges-on-spring are not explicitly treated as additional degrees of freedom, the sum of the forces acting on any charge-on-spring should be zero, and the virtual charge  $q_i^v$  must be positioned such that

$$\vec{f}_i^{\text{ho}} + \vec{f}_i^{\text{coul}} = 0 \quad (8)$$

with the force  $\vec{f}_i^{\text{ho}}$  due to the spring given by

$$\vec{f}_i^{\text{ho}} = -k_i^{\text{ho}}(\vec{r}_i' - \vec{r}_i) = -\frac{(q_i^v)^2}{\alpha_i(4\pi\epsilon_0)}(\vec{r}_i' - \vec{r}_i) \quad (9)$$

and  $\vec{f}_i^{\text{coul}}$  due to the (Coulombic) electric field at the charge-on-spring ( $\vec{E}_i'$ ) given by

$$\vec{f}_i^{\text{coul}} = q_i^v \vec{E}_i' \quad (10)$$

To satisfy eq 8, the  $\vec{\mu}_i$ 's ( $\vec{r}_i$ 's) should be determined from the  $\vec{E}_i'$ 's. However, since the displacement  $|\vec{r}_i' - \vec{r}_i|$  of the charge-on-spring from the polarizable center is nonzero upon polarization, a better approximation of the ideal inducible dipole  $\vec{\mu}_i$  at site  $i$  would be to determine  $\vec{r}_i'$  from the electric field  $\vec{E}_i$  at the polarizable center itself. From eqs 1 and 7, the  $\vec{r}_i$ 's are then determined from

$$\vec{r}_i' = \vec{r}_i + \frac{\alpha_i(4\pi\epsilon_0)\vec{E}_i}{q_i^v} \quad (11)$$

Equations 8–11 show that the total force acting on the charge-on-spring is only zero if

$$\vec{E}_i' = \vec{E}_i \quad (12)$$

which is usually not the case for the induced dipole due to the nonzero values for  $|\vec{r}_i' - \vec{r}_i|$ . By choosing  $q_i^v$  large enough,  $|\vec{r}_i' - \vec{r}_i|$  adopts relatively small values, resulting in small differences between  $\vec{E}_i$  and  $\vec{E}_i'$ . However, the size of  $q_i^v$  is limited to values for which  $|\vec{r}_i' - \vec{r}_i|$  is significant enough with respect to interatomic distances such that numerical precision is ensured when calculating, e.g., interaction energies involving induced dipoles. Like the PPD model, the COS method has been employed in combination with iterative procedures<sup>14</sup> to energy-minimize for the  $\vec{r}_i$ 's (i.e., solving eq 8) or with an extended Lagrangian in which a fictitious mass is assigned to the charge-on-spring and the charges-on-spring are treated as additional degrees of freedom.<sup>15</sup> Originally, a noniterative procedure was proposed,<sup>11</sup> to which the following discussion is of equal importance. In studies using the iterative procedure,  $q_i^v$  was set to  $-8.0 e$ ,<sup>14,16,17</sup> whereas less negative charges were chosen in simulations using a COS model in combination with an extended system Lagrangian (with typical values between  $-1.0$  and  $-2.0 e$ ).<sup>15,18,19</sup> The reason is that in simulations using an extended Lagrangian, the absolute size of  $q_i^v$  is limited by the small simulation time steps that must be taken for large  $|q_i^v|$ , due to the high vibrational frequencies of springs with a large force constant.

In the current work, we quantitatively investigate the error made when calculating the atomic forces according to the version of the charge-on-spring model in which the  $\vec{r}_i$ 's are determined from eq 11, while assuming eq 8 to be fulfilled. For this purpose, calculated values for the components of the atomic electrostatic forces in selected test systems are compared with numerical values for the corresponding finite differences in the electrostatic potential energy. To evaluate the accuracy of the different force calculations, we compare between including contributions from the second term in eq 13

$$\vec{f}_i = -\nabla_i U^{\text{ele}}(\vec{r}, \vec{r}') = -\left( \frac{\partial U^{\text{ele}}}{\partial \vec{r}_i} + \sum_{k \neq i}^N \frac{\partial U^{\text{ele}}}{\partial \vec{r}_k'} \cdot \frac{\partial \vec{r}_k'}{\partial \vec{r}_i} \right) \quad (13)$$

and completely neglecting these contributions (which is equivalent to assuming that eq 8 is satisfied). An expression for  $\sum_{k \neq i}^N (\partial U^{\text{ele}}/\partial \vec{r}_k') \cdot (\partial \vec{r}_k'/\partial \vec{r}_i)$  is derived in section 2. Preferably, the calculation of the contributions from this term is to be avoided in simulations, because it involves tensors of rank two and higher (see section 2), and introducing these terms would reduce the appealing character of the charge-on-spring model when compared to the PPD approach. As an alternative, we investigate whether the size of  $\sum_{k \neq i}^N (\partial U^{\text{ele}}/\partial \vec{r}_k') \cdot (\partial \vec{r}_k'/\partial \vec{r}_i)$  and, hence, the error in the forces when neglecting this term can be satisfactorily reduced by choosing the (absolute) size of the charges-on-spring appropriately

large. Our prime interest is the effect of  $q_i^v$  and the omission of terms involving  $\partial U^{\text{ele}}/\partial \vec{r}_k'$  in the expressions for  $\vec{f}_i$  on the performance of iterative COS models that were recently implemented by us.<sup>14,16,17,20</sup> Therefore, we chose as test systems three gas-phase dimers in which strong dipole–dipole, weak dipolar, or ion–dipole interactions are present, representing interactions typically occurring in biomolecular simulation, in which our COS models are to be used. The effect of the strength of the electric field at the polarizable centers on the results of the calculations is investigated by varying the separation between the monomers, from hydrogen-bonding distance to the typical cutoff distance for electrostatic interactions. From our findings we comment on the optimal choice for  $q_i^v$  and the expression of the atomic forces, thereby considering both the accuracy and consistency of the model and its computational efficiency.

## 2. Theory

Unlike the PPD model, the COS method treats the induced dipole moments via additional point charges only, which allows for an easy introduction of polarizability into schemes to compute long-range electrostatic forces, such as the reaction-field,<sup>21,22</sup> Ewald-summation,<sup>23</sup> Particle–Particle–Particle–Mesh (P3M),<sup>24</sup> and Particle–Mesh–Ewald (PME)<sup>25</sup> techniques. The electrostatic potential  $\phi_i$  at the polarizable centers  $i$  due to the monopoles and dipoles in the system can be expressed using Coulombic terms only

$$\phi_i(\vec{r}, \vec{r}') = \frac{1}{4\pi\epsilon_0} \sum_{j \neq i}^N \left[ \frac{(q_j - q_j^v)}{|\vec{r}_i - \vec{r}_j|} + \frac{q_j^v}{|\vec{r}_i - \vec{r}_j'|} \right] \quad (14)$$

Because of the dependence of the  $\vec{r}_i'$ 's on the  $\vec{r}_j$ 's (and  $\vec{r}_j'$ 's) via  $\vec{E}_i$  in eq 11, the relation between  $\phi_i$  and the electric field  $\vec{E}_i$  is given by

$$\vec{E}_i = -\nabla_i \phi_i(\vec{r}, \vec{r}') = -\left( \frac{\partial \phi_i}{\partial \vec{r}_i} + \sum_{k \neq i}^N \frac{\partial \phi_i}{\partial \vec{r}_k'} \cdot \frac{\partial \vec{r}_k'}{\partial \vec{r}_i} \right) \quad (15)$$

When applying a Born–Oppenheimer-like iterative SCF procedure, however, the  $\vec{r}_i'$ 's are at every iteration step determined in the fixed electric field due to the other  $q_j$ 's and  $q_j^v$ 's. When using a convergence criterion which minimizes the  $\phi_i$ 's with respect to the positions  $\vec{r}_i'$ , the second term in eq 15 is zero at convergence because  $\partial \phi_i / \partial \vec{r}_k' = 0$ . Thus

$$\vec{E}_i = -\frac{\partial \phi_i}{\partial \vec{r}_i} = \frac{1}{4\pi\epsilon_0} \sum_{j \neq i}^N \left[ \frac{(q_j - q_j^v)(\vec{r}_i - \vec{r}_j)}{|\vec{r}_i - \vec{r}_j|^3} + \frac{q_j^v(\vec{r}_i - \vec{r}_j')}{|\vec{r}_i - \vec{r}_j'|^3} \right] \quad (16)$$

The electrostatic part  $U^{\text{ele}}$  of the potential energy can also be expressed in terms of Coulomb interactions. The only non-Coulombic term to be added to  $U^{\text{ele}}$  is the self-polarization energy  $U^{\text{self}}$ , which in the COS model can be expressed in terms involving point charges as well<sup>17</sup>

$$U^{\text{ele}}(\vec{r}, \vec{r}') = U^{\text{coul}} + U^{\text{self}} \quad (17)$$

with

$$U^{\text{coul}}(\vec{r}, \vec{r}') = \frac{1}{4\pi\epsilon_0} \sum_{i=1}^{N-1} \sum_{j>i}^N \left[ \frac{(q_i - q_i^v)(q_j - q_j^v)}{|\vec{r}_i - \vec{r}_j|} + \frac{(q_i - q_i^v)q_j^v}{|\vec{r}_i - \vec{r}_j'|} + \frac{q_i^v(q_j - q_j^v)}{|\vec{r}_i' - \vec{r}_j|} + \frac{q_i^v q_j^v}{|\vec{r}_i' - \vec{r}_j'|} \right] \quad (18)$$

and

$$U^{\text{self}}(\vec{r}, \vec{r}') = \frac{1}{2} \sum_{i=1}^N \frac{(q_i^v)^2}{\alpha_i(4\pi\epsilon_0)} |\vec{r}_i' - \vec{r}_i|^2 \quad (19)$$

Now we consider the expression for the forces  $\vec{f}_i$  that act on (polarizable) atomic centers  $i$

$$\vec{f}_i = -\nabla_i U^{\text{ele}}(\vec{r}, \vec{r}') = -\left( \frac{\partial U^{\text{ele}}}{\partial \vec{r}_i} + \sum_{k \neq i}^N \frac{\partial U^{\text{ele}}}{\partial \vec{r}_k'} \cdot \frac{\partial \vec{r}_k'}{\partial \vec{r}_i} \right) \quad (20)$$

Note again the dependence of the  $\vec{r}_k'$ 's on the  $\vec{r}_i$ 's that appears in the second term on the right in eq 20, which might adopt nonzero values because  $U^{\text{ele}}$  not only contains terms due to the  $\phi_i$ 's (first two terms on the right in eq 18) but also due to the  $\phi_i'$ 's (last two terms on the right in eq 18) and  $U^{\text{self}}$ , whereas when using eq 11 only the  $\phi_i$ 's have been minimized with respect to the  $\vec{r}_i'$ 's. When nevertheless using assumptions 8 and 12, eq 20 reduces to

$$\vec{f}_i^{\text{red}} = -\frac{\partial U^{\text{ele}}}{\partial \vec{r}_i} = -\left( \frac{\partial U^{\text{coul}}}{\partial \vec{r}_i} + \frac{\partial U^{\text{self}}}{\partial \vec{r}_i} \right) \quad (21)$$

From the assumptions in eq 8 and 12 we have

$$-\frac{\partial U^{\text{self}}}{\partial \vec{r}_i} = \vec{f}_i^{\text{ho}} = -\vec{f}_i^{\text{ho}'} = \vec{f}_i^{\text{coul}'} = -\frac{\partial U^{\text{coul}}}{\partial \vec{r}_i'} \quad (22)$$

and the reduced expression  $\vec{f}_i^{\text{red}}$  for the atomic forces becomes<sup>4,14</sup>

$$\vec{f}_i^{\text{red}} = \frac{1}{4\pi\epsilon_0} \sum_{j \neq i}^N \left[ \frac{(q_i - q_i^v)(q_j - q_j^v)(\vec{r}_i - \vec{r}_j)}{|\vec{r}_i - \vec{r}_j|^3} + \frac{(q_i - q_i^v)q_j^v(\vec{r}_i - \vec{r}_j')}{|\vec{r}_i - \vec{r}_j'|^3} + \frac{q_i^v(q_j - q_j^v)(\vec{r}_i' - \vec{r}_j)}{|\vec{r}_i' - \vec{r}_j|^3} + \frac{q_i^v q_j^v(\vec{r}_i' - \vec{r}_j')}{|\vec{r}_i' - \vec{r}_j'|^3} \right] \quad (23)$$

In Appendix A, an expression for the second term on the right in eq 20 is derived up to first order in the many-body electrostatic interactions between polarizable centers and the charges-on-spring, to account for the contribution to the force at atomic center  $i$  originating from the change in the inducible dipoles  $\vec{\mu}_k$ 's ( $\vec{r}_k$ 's) upon a change in  $\vec{r}_i$ . Contributions from higher-order many-body terms have not been calculated explicitly. The first-order terms are to be added to  $\vec{f}_i^{\text{red}}$  to obtain an expression for the first-order corrected force  $\vec{f}_i^{(1)}$

$$\begin{aligned} \vec{f}_i^{(1)} = \vec{f}_i^{\text{red}} + \frac{1}{4\pi\epsilon_0} \sum_{k \neq i} \left[ \sum_{j \neq k} \left( \frac{(q_j - q_j^v)(\vec{r}_j - \vec{r}_k')}{|\vec{r}_j - \vec{r}_k'|^3} + \right. \right. \\ \left. \frac{q_j^v(\vec{r}_j' - \vec{r}_k')}{|\vec{r}_j' - \vec{r}_k'|^3} \right) + \frac{q_k^v}{\alpha_k} (\vec{r}_k' - \vec{r}_k) \cdot \alpha_k \left( (q_i - q_i^v) \left\{ \frac{\vec{I}}{|\vec{r}_i - \vec{r}_k|^3} - \right. \right. \\ \left. \left. \frac{3(\vec{r}_i - \vec{r}_k) \otimes (\vec{r}_i - \vec{r}_k)}{|\vec{r}_i - \vec{r}_k|^5} \right\} + q_i^v \left\{ \frac{\vec{I}}{|\vec{r}_i' - \vec{r}_k|^3} - \right. \right. \\ \left. \left. \frac{3(\vec{r}_i' - \vec{r}_k) \otimes (\vec{r}_i' - \vec{r}_k)}{|\vec{r}_i' - \vec{r}_k|^5} \right\} \right) \left. \right] \quad (24) \end{aligned}$$

with  $\vec{I}$  the three-dimensional unit tensor of second rank. Equation 24 indicates that for infinitely large  $|q_i^v|$ ,  $\vec{f}_i^{(1)}$  will indeed reduce to  $\vec{f}_i^{\text{red}}$ , because the difference between the two terms between curly brackets will vanish as  $(\vec{r}_i' - \vec{r}_k) \rightarrow (\vec{r}_i - \vec{r}_k)$ , and the term involving  $q_k^v/\alpha_k (\vec{r}_k' - \vec{r}_k)$  does not diverge due to the inverse linear dependence of  $(\vec{r}_k' - \vec{r}_k)$  on  $q_k^v$  (eq 11).

### 3. Computational Details

Single-configuration calculations were performed on a water–water, a  $\text{Na}^+$ –water, a  $\text{Na}^+$ – $\text{Cl}^-$ , an argon–water, and an argon– $\text{Na}^+$  dimer, using a version of the GROMOS96 code<sup>26,27</sup> adapted to the charge-on-spring (COS) model.<sup>4,14</sup> Water molecules were described by the polarizable COS/B2 model.<sup>14</sup> In the evaluations of the forces and energies, only nonbonded (and no covalent) interactions were taken into account. Bond constraints were not applied. Nonbonded parameters for  $\text{Na}^+$ ,  $\text{Cl}^-$  and Ar were taken from the GROMOS 43A1 force field,<sup>26</sup> with Ar being polarizable with a polarizability of  $1.6411 \times 10^{-3} \text{ nm}^3$ .<sup>28</sup> The polarizability of the  $\text{Na}^+$  and  $\text{Cl}^-$  ions were either set to zero or to  $1.0 \times 10^{-3} \text{ nm}^3$ . Unless stated otherwise, the charges-on-spring  $q_i^v$  were set to  $-8 e$ .

For the water–water dimer, atomic coordinates corresponded to a  $C_s$ -symmetrical conformation, with covalent bond lengths and angles according to the COS/B2 model<sup>14</sup> (values for the O–H and H–H interatomic (bond) distances are  $r_{\text{OH}} = 0.1 \text{ nm}$  and  $r_{\text{HH}} = 0.163299 \text{ nm}$ ). Dimer configurations were generated by placing the oxygen atoms on the  $x$ -axis and varying the distance between the two oxygen atoms from 0.25 to 1.4 nm (with increments of 0.05 nm). For one of the water molecules, one O–H bond was aligned along the  $x$ -axis, pointing to the oxygen of the other one. The other hydrogen of this water molecule was placed in the  $xy$ -plane. The angle between the  $x$ -axis and the bisector of the bond vectors of the other water molecule was set to  $105.4^\circ$ , and the H–H vector was orthogonal to the  $xy$ -plane, see Figure 1. Configurations for the other dimers were generated by replacing the oxygen of one or both of the water molecules by Ar,  $\text{Na}^+$ , or  $\text{Cl}^-$  and removing the hydrogens attached to the replaced oxygen atom(s). Single-configuration calculations of the electrostatic energies and forces were performed, in which except for the intramolecular interactions all interatomic interactions were taken into account. The convergence criterion<sup>14</sup> for the iterative

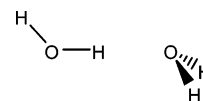


**Figure 1.** Geometry ( $C_s$  symmetry) of the water dimer in the finite-difference calculations. The geometry of the water molecules is described by the COS/B2 model.<sup>14</sup> The O–O distance (which is aligned along the  $x$ -axis) was varied; all other degrees of freedom were kept fixed. The water molecule on the left and the bisector of the water molecule on the right are in the  $xy$ -plane. The angle of this bisector with the  $x$ -axis is  $105.4^\circ$ . The H–H vector of the water molecule on the right is orthogonal to the  $xy$ -plane.

procedure to determine the induced dipoles was

$$\max_{i,x,y,z} (|\Delta E_{i,x}|, |\Delta E_{i,y}|, |\Delta E_{i,z}|) |q_O| |d| < \Delta U \quad (25)$$

with  $\Delta U$  set to  $1 \times 10^{-9} \text{ kJ mol}^{-1}$ . In eq 25,  $d$  is a measure for typical interatomic distances determining the electric field at the polarizable center  $i$  (here we set  $d$  arbitrarily to 1 nm),  $q_O$  was set to the charge of the COS/B2 oxygen ( $-0.746 e$ ), and  $|\Delta E_{i,k}|$  is the change between consecutive iteration steps in the electric field component  $k$  at site  $i$ . The applied criterion not only ensures convergence of the calculated electric field within machine precision but also of the electrostatic potential  $\phi_i$ .

Calculations were performed using expression 23 or 24 for the electrostatic forces at the atomic centers. Components of the electrostatic forces were compared to numerical values obtained from a finite difference in the electrostatic potential energy as calculated after shifting the coordinates of any of the atoms in the  $x$ -,  $y$ -, or  $z$ -direction by  $\Delta x$ ,  $\Delta y$ , or  $\Delta z$  (only the expression for the  $x$ -component is given here)

$$f_{i,x} = \frac{U_{+\Delta x}^{\text{ele}} - U_{-\Delta x}^{\text{ele}}}{2\Delta x} \quad (26)$$

$U_{+\Delta x}^{\text{ele}} (U_{-\Delta x}^{\text{ele}})$  is the electrostatic energy after applying the shift in the positive (negative) direction. Estimated errors in the components of the calculated atomic forces (eqs 23 and 24) are defined as the deviation from the value obtained from eq 26. A value of  $0.5 \times 10^{-5} \text{ nm}$  was chosen for the size of the shifts ( $|\Delta x|$ ,  $|\Delta y|$ , or  $|\Delta z|$ ).

### 4. Results and Discussion

From finite-difference calculations on the nonpolarizable  $\text{Na}^+$ – $\text{Cl}^-$  dimer and the nonpolarizable water dimer with the COS/B2 partial charges scaled by a factor of 0.01 and the atomic polarizabilities of the oxygens ( $\alpha_O$ ) set to zero, we concluded that the length of the shift in the atomic coordinates of  $0.5 \times 10^{-5} \text{ nm}$  is a proper choice for our test systems in order to evaluate whether machine precision can be obtained for the components of the electrostatic forces when compared to finite differences in the Coulombic potential energy. In the case of close contact between the ions (large electrostatic forces and potential-energy values) and of the water molecules with the scaled partial charges at an interatomic distance of 1.4 nm (weak Coulombic interactions), absolute values for the differences between the  $x$ -,  $y$ -, or  $z$ -component of the calculated atomic gradient and



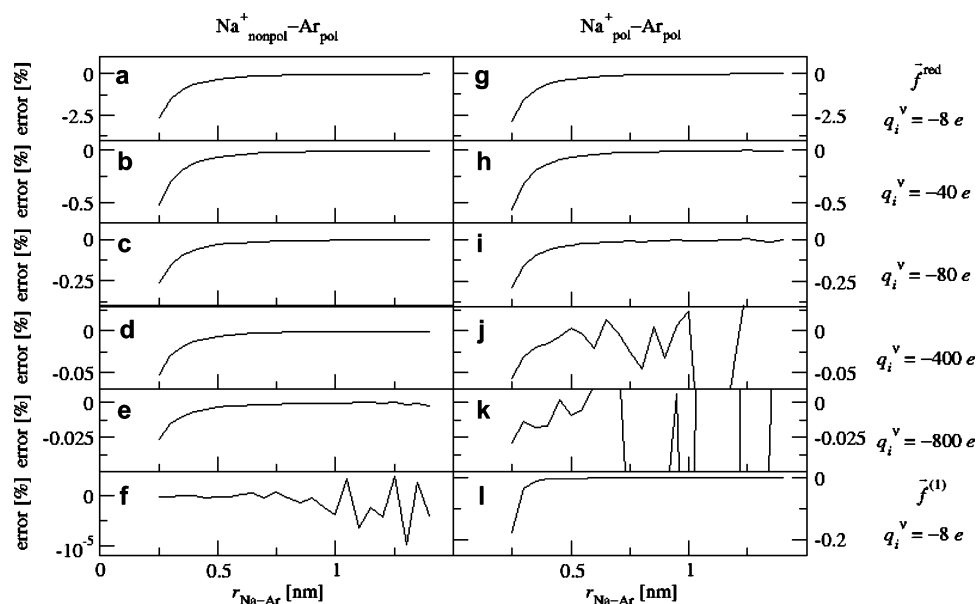


**Figure 2.** Relative error in a single component of the electrostatic atomic force with respect to the corresponding finite difference in the electrostatic potential energy (eq 26) for a gas-phase dimer consisting of a polarizable argon probe and either a nonpolarizable (panels (a)–(f)) or a polarizable (panels (g)–(l))  $\text{Na}^+$  ion, separated by an interatomic distance  $r_{\text{Na-Ar}}$ , where the atomic forces are calculated using eq 23 ( $\vec{f}_i^{\text{red}}$ , panels (a)–(e) and panels (g)–(k)) or using eq 24 ( $\vec{f}_i^{(1)}$ , panels (f) and (l)). In panels (a)–(e), and (g)–(k), the size of the charges-on-spring is varied and set to  $q_i^v = -8 e$ ,  $-40 e$ ,  $-80 e$ ,  $-400 e$ , and  $-800 e$ , respectively. In panels (f) and (l),  $q_i^v = -8 e$ . Note the different scales on the y-axes.

the corresponding finite difference in the energy were maximally in the order of  $10^{-8}\%$  and  $10^{-6}\%$ , respectively. Also for the nonpolarizable COS/B2 ( $\alpha_0 = 0$ ) and  $\text{Na}^+$ –water dimers, machine precision in the calculated force components was obtained, with maximum errors of  $10^{-7}\%$  at any separation distance between the monomers.

In contrast, when considering the electrostatic atomic gradients in the dimers with one or more nonzero polarizabilities, discrepancies with the finite differences in the electrostatic potential energy were found to be larger by several orders of magnitude than for the nonpolarizable dimers. For the  $\text{Na}^+$ –Ar system in which only argon has an inducible dipole moment, e.g., the atomic force  $\vec{f}_i^{\text{red}}$  as calculated from eq 23 (having only one component) differs by  $-0.015\%$  from the negative of the finite-difference in the electrostatic energy when the distance between the sodium ion and the argon atom ( $r_{\text{Na-Ar}}$ ) is 1.4 nm, and by no less than  $-2.7\%$  for  $r_{\text{Na-Ar}} = 0.25$  nm, see Figure 2a. Machine precision is recovered by evaluating  $\vec{f}_i^{(1)}$  (using eq 24) instead of  $\vec{f}_i^{\text{red}}$ . Figure 2f shows that the errors in  $\vec{f}_i^{(1)}$  are typically  $10^{-6}$  or  $10^{-5}\%$ . The significant error in the calculated forces when using the reduced expression 23 can be explained from the neglect of the contribution to the atomic forces that is due to the change in the electric field at argon and, hence, its inducible dipole upon a displacement of  $\text{Na}^+$  or Ar. This effect is accounted for by the first-order correction terms in eq 24. The decay of the relative error in  $\vec{f}_i^{\text{red}}$  with increasing  $r_{\text{Na-Ar}}$  (Figure 2a) can be explained from the corresponding decrease in the size of the correction factor in eq 24 which scales with  $(r_{\text{Na-Ar}})^{-3}$ , whereas  $\vec{f}_i^{\text{red}}$  scales with  $(r_{\text{Na-Ar}})^{-2}$ .

In the presence of a single polarizable center, the first-order correction on  $\vec{f}_i^{\text{red}}$  suffices to obtain machine precision

in the calculated electrostatic gradients (Figure 2f). However, when considering a  $\text{Na}^+$ –Ar dimer in which both the argon and the ion are polarizable (from hereon referred to as  $\text{Na}^+_{\text{pol}}\text{-Ar}_{\text{pol}}$ ), we observe discrepancies not only between the finite differences in the electrostatic potential energies with calculated values for  $\vec{f}_i^{\text{red}}$  (see Figure 2g) but also with calculated values for  $\vec{f}_i^{(1)}$ , see Figure 2l. The reason is that in the presence of more than one polarizable center, higher-order many-body effects come into play. A change in dipole induction of Ar ( $\text{Na}^+$ ) due to a displacement of  $\text{Na}^+$  (Ar) leads again to a change in polarization of the ion (argon probe) itself, and terms accounting for this second-order many-body effect have been neglected in deriving  $\vec{f}_i^{(1)}$  (Appendix A). The error in  $\vec{f}_i^{(1)}$  calculated for the  $\text{Na}^+_{\text{pol}}\text{-Ar}_{\text{pol}}$  dimer at short  $r_{\text{Na-Ar}}$  is an order of magnitude smaller than the error in  $\vec{f}_i^{\text{red}}$ , but its maximal value of 0.2% is still significant (see Figure 2l). Because the second-order correction terms on  $\vec{f}_i^{\text{red}}$  that are missing in  $\vec{f}_i^{(1)}$  inversely scale with a larger exponent in  $r_{\text{Na-Ar}}$  than the terms in  $\vec{f}_i^{(1)}$ , errors in  $\vec{f}_i^{(1)}$  for the  $\text{Na}^+_{\text{pol}}\text{-Ar}_{\text{pol}}$  dimer with  $r_{\text{Na-Ar}}$  approximating 1.4 nm come close to the limit of machine precision, with values on the order of  $10^{-4}\%$ . However, in condensed-phase simulations, close neighbor interactions will screen long-range interactions and will dominate the size and error of the atomic gradients. Note that for  $\text{Na}^+_{\text{pol}}\text{-Ar}_{\text{pol}}$ , errors in  $\vec{f}_i^{\text{red}}$  are of similar magnitude when compared to the case in which the sodium ion was not polarizable (compare parts a and g of Figure 2), because of the small contribution of the induced dipole at  $\text{Na}^+$  to the total electrostatic interactions which are dominated by the (fixed) net charge of the ion.

For the  $\text{Na}^+_{\text{pol}}\text{-Ar}_{\text{pol}}$  dimer, observed differences between the components of  $\vec{f}_i^{\text{red}}$  and  $\vec{f}_i^{(1)}$  and the corresponding finite

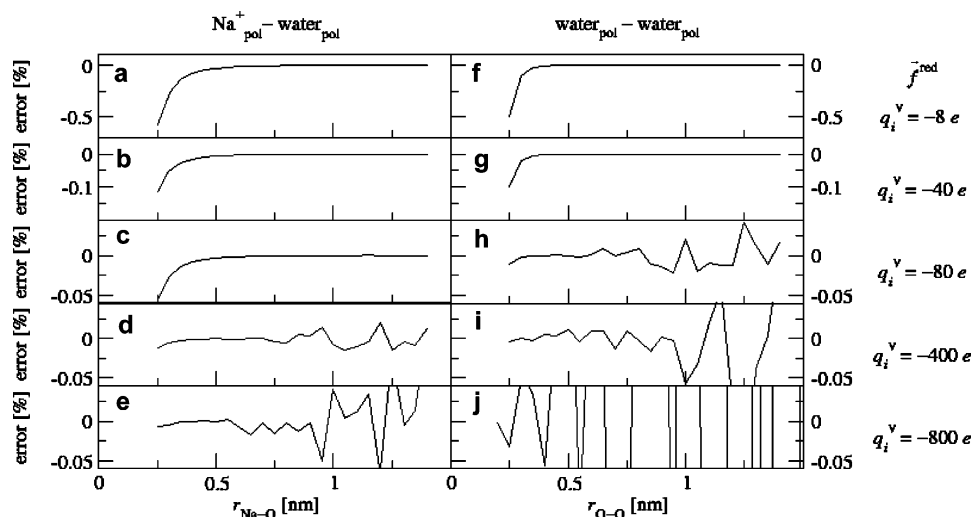


**Figure 3.** Relative error in the  $x$ -component of the electrostatic force at  $\text{Na}^+$  or at the water oxygen, with respect to the corresponding finite difference in the electrostatic potential energy (eq 26) for a gas-phase dimer consisting of a COS/B2 water molecule and a polarizable  $\text{Na}^+$  ion (panels (a)–(e)) or two COS/B2 water molecules (panels (f)–(j)), separated by an interatomic distance ( $r_{\text{Na-O}}$  and  $r_{\text{O-O}}$ , respectively), where the atomic forces are calculated using eq 23 ( $\vec{f}_i^{\text{red}}$ ). In panels (a)–(e), and (f)–(j), the size of the charges-on-spring is varied and set to  $q_i^v = -8 e$ ,  $-40 e$ ,  $-80 e$ ,  $-400 e$ , and  $-800 e$ , respectively. Note the different scales on the  $y$ -axes.

differences in the electrostatic energies are relatively large when compared to the situation of the  $\text{Na}^+$ –water or  $\text{Na}^+$ – $\text{Cl}^-$  dimers in which both monomers are polarizable as well. Because electrostatic interactions between  $\text{Na}^+$  and argon are only due to interactions involving the induced dipole on argon, relative contributions from the terms due to  $\sum_{k \neq i}^N (\partial U^{\text{ele}} / \partial \vec{r}_k') \cdot (\partial \vec{r}_k' / \partial \vec{r}_i)$  in eq 13 sum up to the total error in the electrostatic forces when calculated for  $\vec{f}_i^{\text{red}}$ . When going from the  $\text{Na}^+$ –Ar system to the  $\text{Na}^+$ –water or the  $\text{Na}^+$ – $\text{Cl}^-$  dimer, in which apart from ion-induced dipole interactions, ion-fixed dipole or ion–ion interactions are present, we observe a significant decrease in the relative errors in calculated values for  $\vec{f}_i^{(1)}$  and  $\vec{f}_i^{\text{red}}$  at  $\text{Na}^+$  (which have again a single ( $x$ )-component). At close distance between the (polarizable) monomers, the error in  $\vec{f}_i^{\text{red}}$  at  $\text{Na}^+$  is one or several orders of magnitude smaller for  $\text{Na}^+$ –water ( $-0.6\%$ ) or  $\text{Na}^+$ – $\text{Cl}^-$  ( $-0.003\%$ ) than for  $\text{Na}^+_{\text{pol}}$ – $\text{Ar}_{\text{pol}}$  ( $-2.9\%$ ). Moreover, at maximal separation between the monomers, machine precision in the components of the atomic forces when calculated from eq 23 is obtained for  $\text{Na}^+$ –water (Figure 3a) and  $\text{Na}^+$ – $\text{Cl}^-$  (results not shown). The reason is that the contribution to the forces from the fixed charge distributions is correctly computed (as is apparent from our finite-difference calculations on the nonpolarizable dimers), and the contribution to the total forces from the fixed point charge distribution is usually larger than the contribution from the inducible dipoles, especially in case of large separation distance between the monomers (due to small local electric fields and accordingly small induced dipoles) or ion–ion interactions.

When considering dimers such as the water–argon and water–water systems, in which interactions involving ionic species are not present, the smaller electric fields at the polarizable centers compared to when ions are present cause a smaller induction of the inducible dipoles, and the assumption in eq 12 (and in eq 8) is more justified. On the

other hand, in the presence of an ion, the many-body contributions from the induced dipole moment on the neutral monomer is the main source of errors in  $\vec{f}_i^{\text{red}}$  (compare parts a and g of Figure 2). When going to dimers with neutral monomers solely, there is a doubling of the number of the error sources. For the fully polarizable water–argon (results not shown) and water–water dimer (Figure 3f), these effects apparently counteract such that deviations of the components of the  $\vec{f}_i^{\text{red}}$ 's at oxygen and argon from the corresponding finite differences in the electrostatic potential energy are comparable to the errors in  $\vec{f}_i^{\text{red}}$  in the case of  $\text{Na}^+$ –argon (Figure 2g) and  $\text{Na}^+$ –water (Figure 3a), respectively.

From the above it is clear that contributions from  $\sum_{k \neq i}^N (\partial U^{\text{ele}} / \partial \vec{r}_k') \cdot (\partial \vec{r}_k' / \partial \vec{r}_i)$  in eq 13 can adopt significant values. Furthermore, if a first-order correction on the reduced expression for the atomic forces in eq 23 is taken into account (using expression 24), errors in the calculated forces decrease but are still found to be significant in the presence of more than one polarizable center in the system. Including the first-order correction terms in eq 24 makes the calculation of the forces already more expensive compared to the evaluation of  $\vec{f}_i^{\text{red}}$ , and the number of terms in the higher-order corrections rapidly increases due to the third term on the right in eq A2 and the second term on the right in eq A3, which contain tensors of third rank and higher. With an eye to the computational efficiency of the charge-on-spring model, it is not an option to take these terms into account in molecular dynamics simulations. As an alternative, we investigate here to which extent errors in the atomic forces (as a result of completely neglecting  $\sum_{k \neq i}^N (\partial U^{\text{ele}} / \partial \vec{r}_k') \cdot (\partial \vec{r}_k' / \partial \vec{r}_i)$  in eq 13) can be minimized by choosing an appropriately large (absolute) value for the charge-on-spring  $q_i^v$ .

Figures 2 and 3 show errors in the calculated values for the atomic gradients in the polarizable  $\text{Na}^+$ –Ar,  $\text{Na}^+$ –water,

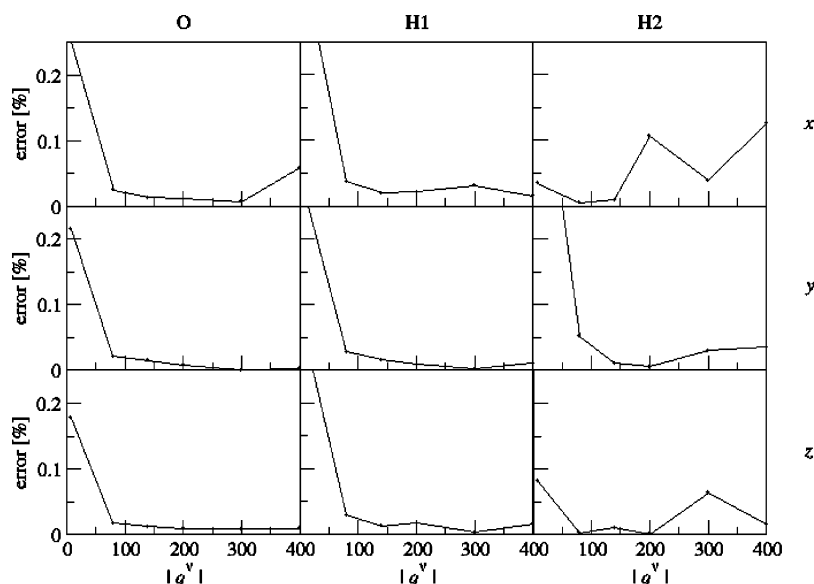


**Figure 4.** Absolute value of the relative error in the  $x$ -,  $y$ -, and  $z$ -component (upper, middle, and lower panels, respectively) of the electrostatic force (calculated using eq 23) at the oxygen (left panels), first hydrogen (middle panels), or second hydrogen atom (right panels) of a randomly chosen water molecule in a periodic box filled with 1000 COS/B2 water molecules, with respect to the corresponding finite differences in the electrostatic potential energy (eq 26), for different absolute values for the charge-on-spring  $q_i^v$ .

and water–water dimers with respect to the finite difference in the electrostatic energy for different values of the charges-on-spring, varying from  $-8 e$  to  $-800 e$ . For the polarizable dimers considered, the discrepancy between the components of  $\vec{f}_i^{\text{red}}$  and the corresponding finite differences in the electrostatic potential energy is found to inversely scale down with  $|q_i^v|$  in case of close contact between the monomers (see Figures 2 and 3). However, at large separation distance between the monomers and from  $q_i^v = -80 e$  onward, the relative error in  $\vec{f}_i^{\text{red}}$  rapidly increases with  $q_i^v$  adopting more negative values. The reason is that at large separation distance between the monomers, the  $\vec{E}_i$ 's adopt small values and the displacements  $|\vec{r}_i' - \vec{r}_i|$  of the charges-on-spring become relatively small compared to interatomic distances  $|\vec{r}_i - \vec{r}_j|$ . As a result,  $|\vec{r}_i' - \vec{r}_i|$  values are not significant enough anymore, resulting in an inaccurate determination of  $\vec{f}_i^{\text{red}}$  (and  $\vec{f}_i^{(1)}$  as well, results not shown). This effect is most pronounced for the water dimer (Figure 3f–j), because the dipole–dipole interactions within this dimer scale with  $|\vec{r}_i - \vec{r}_j|^{-3}$  instead of  $|\vec{r}_i - \vec{r}_j|^{-2}$  as the ion–dipole interactions do in the case of  $\text{Na}^+$  being present (Figures 2 and 3a–e). The error in  $\vec{f}_i^{\text{red}}$  for large  $|q_i^v|$  and separation distance between the monomers is also more pronounced for  $\text{Na}^+_{\text{pol}} - \text{Ar}_{\text{pol}}$  and  $\text{Na}^+_{\text{pol}} - \text{water}$  than for the  $\text{Na}^+ - \text{Ar}$  dimer in which only the argon probe is polarizable. In the latter case, dipole induction is only due to the electric field generated by a net charge which only scales with  $|\vec{r}_i - \vec{r}_j|^{-2}$ , resulting in values for  $|\vec{r}_i' - \vec{r}_i|$  that are even significant at maximal separation between the monomers.

From the above, effectively reducing errors in  $\vec{f}_i^{\text{red}}$  (and  $\vec{f}_i^{(1)}$ ) through choosing large values for  $|q_i^v|$  is limited in the situation of the gas-phase dimers, because of inaccuracies introduced in evaluating long-range forces due to dipolar interactions. However, our COS models<sup>14,16,17,20</sup> were developed for use in condensed-phase simulations, and solvent

screening will significantly affect long-range interactions. To quantify the effect of solvent screening on errors in the reduced force  $\vec{f}_i^{\text{red}}$ , we repeated the calculations on our test systems for a randomly picked water molecule out of configurations consisting of 1000 COS/B2 water molecules in a cubic periodic box with a volume of  $29.616 \text{ nm}^3$ . (The system was equilibrated in a NVT molecular dynamics simulation at 298.15 K. Nonbonded interactions were calculated for water molecules which were within 1.4 nm, and no long-range correction for the long-range nonbonded interactions was applied.) Whereas machine precision was obtained in the evaluation of the forces when all atomic polarizabilities are set to zero (results not shown), significant errors are observed for the components of  $\vec{f}_i^{\text{red}}$  at the atoms from calculations on the polarizable system. Figure 4 shows trends in the error in the  $x$ -,  $y$ -, and  $z$ -components of  $\vec{f}_i^{\text{red}}$  for the oxygen and hydrogen atoms for the selected water molecule upon varying  $q_i^v$  from values of  $-8 e$  up till  $-400 e$ . As in the case of the gas-phase dimer consisting of two COS/B2 water molecules at close contact (see Figure 3f), the error in  $\vec{f}_i^{\text{red}}$  is a few tenths of a percent for  $q_i^v = -8 e$ . Also the finding that this error reduces by increasing  $|q_i^v|$  to values of up to  $-200 e$  (see Figure 4) indicates that short-range interactions determine the total force acting on the particle. We found the error in the long-range forces to increase for the dimeric  $\text{water}_{\text{pol}} - \text{water}_{\text{pol}}$  system when going, for example, from  $q_i^v = -40 e$  to  $q_i^v = -80 e$ . From Figure 4, the error in the components of  $\vec{f}_i^{\text{red}}$  at the atoms is in most cases minimal at  $q_i^v = -200 e$  or  $q_i^v = -300 e$ . In many cases, an increase in the error is observed when going from  $q_i^v = -300 e$  to  $q_i^v = -400 e$ , probably due to too small  $|\vec{r}_i' - \vec{r}_i|$  values relative to interatomic distances. Similar trends were observed when calculating  $\vec{f}_i^{\text{red}}$  at  $\text{Na}^+$  or Ar after removing the selected water molecule from the system and

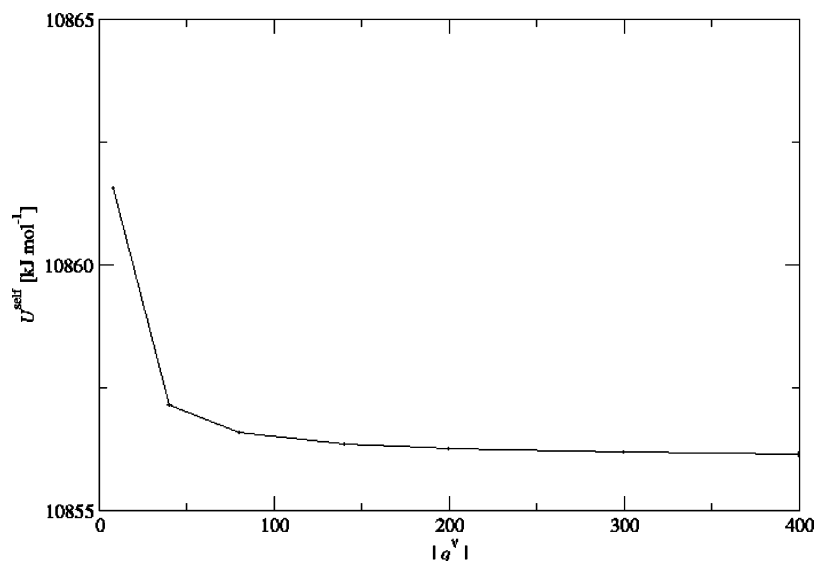


**Figure 5.** Total self-polarization energy  $U^{\text{self}}$  (eq 19) for a periodic box filled with 1000 COS/B2 water molecules for different absolute values for the charge-on-spring  $q_i^v$ .

placing a polarizable  $\text{Na}^+$  or argon probe at the position of its oxygen atom (results not shown). Only the error in the  $x$ -component of  $\vec{f}_i^{\text{red}}$  at one of the hydrogen atoms of the water molecule is minimal at a less negative value for  $q_i^v$  than  $-200 e$ . The reason is that this component of  $\vec{f}_i^{\text{red}}$  is by 1 or 2 orders of magnitude smaller than the other components in the water molecule, making its determination intrinsically less accurate. Upon choosing  $q_i^v = -200 e$  or  $q_i^v = -300 e$ , relative errors in  $\vec{f}_i^{\text{red}}$  at  $\text{Na}^+$ , argon, and the atoms in water are typically up to 2 orders of magnitude smaller when compared to using a value of  $-8 e$  for  $q_i^v$ . Note that not only the error in  $\vec{f}_i^{\text{red}}$  is affected by  $q_i^v$  but also the total electrostatic energy, as reflected by the self-polarization energy  $U^{\text{self}}$  (see Figure 5 for the pure water box).  $U^{\text{self}}$  is (from linear response theory) a direct measure for the total contribution of the induced dipoles to the potential energy of the system and is for relatively small values for  $|q_i^v|$  not converging to the value that would be obtained in the case of treating the induced dipoles as being infinitely small. However, the total variation of  $U^{\text{self}}$  with respect to  $q_i^v$  for  $|q_i^v| \geq 40 e$  is small when compared to  $k_B T (=2.5 \text{ kJ mol}^{-1}$  at 298.15 K), see Figure 5. It would be interesting to see if using a value of  $q_i^v = -200 e$  or  $-300 e$  instead of  $-8 e$  in combination with expression 23 for the forces leads not only to a better description of the (reduced) atomic forces and self-polarization energy but also to an improvement in describing other relevant properties of condensed-phase systems, such as the dielectric permittivity of polar liquids which was found to be significantly off from experiment for COS-based solvent models that were recently developed in our group.<sup>14,16,17,20</sup> This will be the subject of a future molecular dynamics simulation study by us. In addition, the effect on various liquid properties of using expression 24 for  $\vec{f}_i^{(1)}$  instead of expression 23 for the atomic forces in simulations of polarizable liquids will be evaluated. From calculations on  $\vec{f}_i^{\text{red}}$  and  $\vec{f}_i^{(1)}$  for the randomly picked water molecule in the COS/B2 water box with  $q_i^v$  set to  $-200 e$ , use of the expression for  $\vec{f}_i^{(1)}$  was found to additionally

reduce deviations with finite differences in the potential energy by 1 order of magnitude (results not shown).

In simulations using an extended Lagrangian in combination with the COS model, the first-order correction in eq 24 (due to  $\sum_{k \neq i}^N (\partial U^{\text{ele}} / \partial \vec{r}_k') \cdot (\partial \vec{r}_k' / \partial \vec{r}_i)$  in eq 13) does in principle not have to be considered due to the explicit treatment of the charges-on-spring as degrees of freedom. However, simulation settings are usually<sup>15,29</sup> chosen such that the charges-on-spring follow the Born–Oppenheimer dipole interaction energy surface according to the atomic coordinates, making the  $\vec{r}_i'$ 's implicitly depending on the set of  $\vec{r}_i$ 's. It would be interesting to evaluate contributions from this dependence of  $\vec{r}_i'$  on  $\vec{r}_i$  to the forces and electric fields in simulations using an extended Lagrangian, which might be large because  $q_i^v$  is usually set to relative small values to reduce the vibrational frequencies of the charges-on-spring. For the  $\text{Na}^+$ –argon dimer, for example, the difference between  $\vec{f}_i^{\text{red}}$  and the finite difference in the electrostatic potential energy was found to add up to  $-12\%$  when  $q_i^v = -2 e$  is chosen, as in ref 15. From the discussion in section 1, the contribution of  $\sum_{k \neq i}^N (\partial U^{\text{ele}} / \partial \vec{r}_k') \cdot (\partial \vec{r}_k' / \partial \vec{r}_i)$  will be zero upon replacing  $\vec{E}_i$  in eq 11 by  $\vec{E}_i'$  as Lamoureux and Roux did in their implementation of the charge-on-spring model using an extended Lagrangian.<sup>15</sup> Indeed, with an adapted version of the polarizable GROMOS96 code in which the inducible dipoles were determined from  $\vec{E}_i'$  instead of  $\vec{E}_i$ , machine precision was obtained in the reduced force  $\vec{f}_i^{\text{red}}$  when compared to the finite difference in the electrostatic energy (results not shown).

Finally, we note that in the PPD model, the correction term to be added to the ‘reduced’ atomic forces (due to the second term on the right in eq 3) is zero when applying an iterative SCF procedure, because of the infinitely small size of the induced dipoles. However, as pointed out by Rick and Stuart already,<sup>2</sup> this does not make the PPD model physically more realistic than the COS model: treating electron polarization effects by inducible dipoles of finite size might even be considered a better representation of the



(noninfinitely small) electron clouds which in quantum-mechanically treated systems cause the corresponding induced dipoles.

## 5. Conclusions

When using the charge-on-spring model to explicitly account for electronic polarization and calculating the induced dipole at a polarizable center from the electric field at the polarizable center itself (i.e., using eq 11), a contribution to the atomic forces arises due to the dependence of the positions of the charges-on-spring on the positions of all other point charges (second term on the right in eq 13). For a system with a single polarizable center, this contribution can be accounted for by adding a first-order correction to the reduced atomic force  $\vec{f}_i^{\text{red}}$  which neglects this effect (eq 23). However, we found that higher-order corrections are to be included for systems with more than one charge-on-spring in order to obtain machine precision in the calculated atomic forces. These higher-order corrections contain second- and higher-rank tensors and make the evaluation of the forces cumbersome and time-consuming. As an alternative, the error in calculating the atomic forces introduced via neglecting the second term on the right in eq 13 can be minimized by choosing the size of the charge-on-spring  $q_i^v$  appropriately large, thereby minimizing the finite size of the induced dipoles. From the evaluation of the force at atoms of a water molecule, at argon, or at  $\text{Na}^+$  solvated in a box of water, with the system described by a polarizable force field, we found that components of  $\vec{f}_i^{\text{red}}$  are closest to the finite difference in the Coulombic energy, upon setting  $q_i^v$  to  $-200 e$  or  $-300 e$ . Work is under way to quantify the effect of using this value for  $q_i^v$  (instead of  $-8 e$  as in previous molecular dynamics simulation studies) on the properties of condensed-phase systems as determined from simulation using the charge-on-spring model.

## Appendix A

To derive an expression for  $\sum_{k \neq i}^N (\partial U^{\text{ele}} / \partial \vec{r}_k') \cdot (\partial \vec{r}_k' / \partial \vec{r}_i)$ , we consider in the following the two partial derivatives separately. First

$$\frac{\partial U^{\text{ele}}}{\partial \vec{r}_k'} = \frac{\partial U^{\text{coul}}}{\partial \vec{r}_k'} + \frac{\partial U^{\text{self}}}{\partial \vec{r}_k'} \quad (\text{A1})$$

with, from eq 18 and by taking the dependence of the other  $\vec{r}_m''$ s on  $\vec{r}_k'$  into account

$$\frac{\partial U^{\text{coul}}}{\partial \vec{r}_k'} = \frac{1}{4\pi\epsilon_0} \sum_{j \neq k}^N \left( \frac{(q_j - q_i^v) q_k^v (\vec{r}_j - \vec{r}_k')}{|\vec{r}_j - \vec{r}_k'|^3} + \frac{q_j^v q_k^v (\vec{r}_j' - \vec{r}_k')}{|\vec{r}_j' - \vec{r}_k'|^3} + \sum_{m \neq k}^N \frac{\partial U^{\text{coul}}}{\partial \vec{r}_m'} \cdot \frac{\partial \vec{r}_m'}{\partial \vec{r}_k'} \right) \quad (\text{A2})$$

and from eq 19

$$\frac{\partial U^{\text{self}}}{\partial \vec{r}_k'} = \frac{(q_k^v)^2 (\vec{r}_k' - \vec{r}_k)}{\alpha_k 4\pi\epsilon_0} + \sum_{m \neq k}^N \frac{\partial U^{\text{self}}}{\partial \vec{r}_m'} \cdot \frac{\partial \vec{r}_m'}{\partial \vec{r}_k'} \quad (\text{A3})$$

Second, using eq 11 we find for  $i \neq k$

$$\frac{\partial \vec{r}_k'}{\partial \vec{r}_i} = \frac{\alpha_k (4\pi\epsilon_0)}{q_k^v} \left( \frac{\partial \vec{E}_k}{\partial \vec{r}_i} + \sum_{m \neq k}^N \frac{\partial \vec{E}_k}{\partial \vec{r}_m'} \cdot \frac{\partial \vec{r}_m'}{\partial \vec{r}_i} \right) \quad (\text{A4})$$

where using eq 16 and for  $i \neq k$

$$\frac{\partial \vec{E}_k}{\partial \vec{r}_i} = -\frac{(q_i - q_i^v)}{4\pi\epsilon_0} \left\{ \frac{\vec{I}}{|\vec{r}_i - \vec{r}_k|^3} - \frac{3(\vec{r}_i - \vec{r}_k) \otimes (\vec{r}_i - \vec{r}_k)}{|\vec{r}_i - \vec{r}_k|^5} \right\} \quad (\text{A5})$$

and

$$\frac{\partial \vec{E}_k}{\partial \vec{r}_i'} = -\frac{q_i^v}{4\pi\epsilon_0} \left\{ \frac{\vec{I}}{|\vec{r}_i' - \vec{r}_k|^3} - \frac{3(\vec{r}_i' - \vec{r}_k) \otimes (\vec{r}_i' - \vec{r}_k)}{|\vec{r}_i' - \vec{r}_k|^5} \right\} \quad (\text{A6})$$

Neglecting the third term on the right in eq A2 and the second term on the right in eq A3 and keeping only the terms  $m = i \neq k$  in the summation in eq A4, eqs 20, 23, and A1–A6 yield the first-order corrected expression for the atomic force on  $i$ ,  $\vec{f}_i^{(1)}$ , as given in eq 24.

**Acknowledgment.** The authors thank Anna-Pitschna Kunz and Merijn Schenk for helpful discussions. Financial support from the National Center of Competence in Research (NCCR) in Structural Biology and from grant number 200021-109227 of the Swiss National Science Foundation is gratefully acknowledged.

## References

- (1) Halgren, T. A.; Damm, W. *Curr. Opin. Struct. Biol.* **2001**, *11*, 236.
- (2) Rick, S. W.; Stuart, S. J. Potentials and algorithms for incorporating polarizability in computer simulations. In *Reviews in Computational Chemistry*; 2002; Vol. 18, p 89.
- (3) Ponder, J. W.; Case, D. A. *Adv. Prot. Chem.* **2003**, *66*, 27.
- (4) Yu, H. B.; van Gunsteren, W. F. *Comput. Phys. Commun.* **2005**, *172*, 69.
- (5) Warshel, A.; Levitt, M. *J. Mol. Biol.* **1976**, *103*, 227.
- (6) Vesely, F. J. *J. Comput. Phys.* **1977**, *24*, 361.
- (7) Van Belle, D.; Couplet, I.; Prevost, M.; Wodak, S. J. *J. Mol. Biol.* **1987**, *198*, 721.
- (8) Berendsen, H. J. C.; Grigera, J. R.; Straatsma, T. P. *J. Phys. Chem.* **1987**, *91*, 6269.
- (9) Born, M.; Oppenheimer, R. *Ann. Phys. (Leipzig)* **1927**, *84*, 457.
- (10) Car, R.; Parrinello, M. *Phys. Rev. Lett.* **1985**, *55*, 2471.
- (11) Straatsma, T. P.; McCammon, J. A. *Mol. Simul.* **1990**, *5*, 181.
- (12) Drude, P. *The Theory of Optics*; Longmans, Green, and Co.: New York, 1902.
- (13) Born, M.; Huang, K. *Dynamic Theory of Crystal Lattices*; Oxford University Press: Oxford, U.K., 1954.
- (14) Yu, H. B.; Hansson, T.; van Gunsteren, W. F. *J. Chem. Phys.* **2003**, *118*, 221.

- (15) Lamoureux, G.; Roux, B. *J. Chem. Phys.* **2003**, *119*, 3025.
- (16) Yu, H. B.; van Gunsteren, W. F. *J. Chem. Phys.* **2004**, *121*, 9549.
- (17) Yu, H. B.; Geerke, D. P.; Liu, H. Y.; van Gunsteren, W. F. *J. Comput. Chem.* **2006**, *27*, 1494.
- (18) Lamoureux, G.; MacKerell, A. D.; Roux, B. *J. Chem. Phys.* **2003**, *119*, 5185.
- (19) Anisimov, V. M.; Lamoureux, G.; Vorobyov, I. V.; Huang, N.; Roux, B.; MacKerell, A. D. *J. Chem. Theory Comput.* **2005**, *1*, 153.
- (20) Geerke, D. P.; van Gunsteren, W. F. *Mol. Phys.* **2007**, DOI: 10.1080/00268970701444631.
- (21) Barker, J. A.; Watts, R. O. *Mol. Phys.* **1973**, *26*, 789.
- (22) Tironi, I. G.; Sperb, R.; Smith, P. E.; van Gunsteren, W. F. *J. Chem. Phys.* **1995**, *102*, 5451.
- (23) Ewald, P. P. *Ann. Phys.* **1921**, *64*, 253.
- (24) Hockney, R. W.; Eastwood, J. W. *Computer Simulation using Particles*, 2nd ed.; Institute of Physics Publishing: Bristol, U.K., 1988.
- (25) Darden, T.; York, D.; Pedersen, L. *J. Chem. Phys.* **1993**, *98*, 10089.
- (26) van Gunsteren, W. F.; Billeter, S. R.; Eising, A. A.; Hünenberger, P. H.; Krüger, P.; Mark, A. E.; Scott, W. R. P.; Tironi, I. G. *Biomolecular Simulation: The GROMOS96 Manual and User Guide*; vdf Hochschulverlag: ETH Zürich, Switzerland, 1996.
- (27) Scott, W. R. P.; Hünenberger, P. H.; Tironi, I. G.; Mark, A. E.; Billeter, S. R.; Fennen, J.; Torda, A. E.; Huber, T.; Krüger, P.; van Gunsteren, W. F. *J. Phys. Chem. A* **1999**, *103*, 3596.
- (28) *CRC Handbook of Chemistry and Physics*, 82th ed.; Lide, D. R., Ed.; CRC Press: Boca Raton, FL, 2001–2002.
- (29) Sprik, M. *J. Phys. Chem.* **1991**, *95*, 2283.

CT700164K